Power spectrum of density fluctuations in a finite reactive-diffusive system: resistance fluctuation spectroscopy

V BALAKRISHNAN and N K BANSAL*

Reactor Research Centre, Kalpakkam 603 102
*Permanent address: St. Stephen's College, University of Delhi, Delhi 110 007

Abstract. The measurement in thermal equilibrium of the vacancy contribution to the residual resistivity of metals has posed certain difficulties. The recent experiment of Celasco and co-workers represents a new, powerful approach to this problem, via the measurement of the power spectrum of the voltage noise generated by resistivity fluctuations. The latter originate in vacancy number fluctuations. We develop a theory for the power spectrum, incorporating three basic features. Vacancies can be annihilated in the material and they diffuse. Grain boundaries act as sources and sinks for vacancies. Both annihilation (a form of reaction) and diffusion are noisy processes. We therefore set up and solve a reactive-diffusive stochastic equation for the instantaneous density, with appropriate *finite* boundary conditions. Assuming for simplicity that the grains are spherical, the power spectrum is evaluated exactly, in closed form. A detailed comparison with experiment is made. The physical origins of different time scales in the problem and the consequent frequency regimes in the power spectrum are analysed. Recognising the very general applicability of our theory, we also mention possible applications to other problems.

Keywords. Resistivity; fluctuations; vacancies; reactive-diffusive system; power spectrum.

1. Introduction

The measurement of the vacancy contribution to the residual resistivity of a metal presents certain special problems. At low temperatures ($T/T_M \ll 1$, where T_M is the melting point), the equilibrium concentration of vacancies is too low for satisfactory measurements to be made. The concentration is therefore artificially built up and the defects are frozen in, for example by quenching from a high T, before measurements are made at low T. This implies, of course, non-equilibrium conditions in the thermodynamic sense. The subsequent extraction of information on thermodynamic quantities of interest such as the vacancy activation energy and the entropy of formation is not straightforward, and requires further assumptions. Experiments *have* been performed under equilibrium conditions (see the references in Celasco *et al* 1976), but they involve measuring the resistivity of the metal right upto T_M and then subtracting the estimated resistivity of the perfect crystal. The weakness of this last procedure has been brought out by Seeger (1973). It is therefore necessary to look for an alternative experimental method that permits measurement in thermal equilibrium and yields a value for the vacancy contribution to resistivity in a reasonably unambiguous manner.

481

This is precisely the problem that has been solved in the experiment of Celasco *et al* (1976) (referred to as CFM hereafter). A careful measurement has been made of the *power spectrum* of the current noise generated by vacancy number fluctuations in a small specimen of aluminium at relatively high temperatures: 435°C or $T/T_M = 0.76$, and 475°C or $T/T_M = 0.80$. The experimental set-up involved a bridge circuit and cross-correlation techniques, and eliminated the large but flat Johnson noise component, amplifier noise, electromigration effects, etc. Spectral analysis could be carried out with a remarkable sensitivity, as fine as 5×10^{-21} V^2/Hz right down to 5 Hz. At the upper end, the power spectrum was measurable upto frequencies of the order of 10^2 Hz. Two distinct components were observed in the power spectrum at each temperature, as shown in figure 1. At low frequencies ($\approx$ 7–20 Hz), the power spectrum is roughly linear in a log-log plot, with a slope approximately equal to -2. There is an ankle in the region 20–40 Hz, beyond which the spectrum resumes linearity, but with a slope ≈ -1.6. It turns out that the latter component is the one that arises from the monovacancy contribution to the resistivity. (CFM also observe that some other mechanism, possibly the scattering from vacancy clusters, must be responsible for the low-frequency component.) If one envisages a simple shot-noise like model, in which each vacancy contributes a constant ' pulse ' of resistance $\triangle R$ during its lifetime τ, it is easy to work out the consequent power spectrum. A constant current I is maintained in the sample. Each vacancy therefore contributes a voltage pulse of height $I \triangle R$ during its lifetime. Let these pulses occur at a rate ν per second. The Fourier transform of the autocorrelation of the voltage fluctuation, i.e., the voltage power spectrum, is then given by

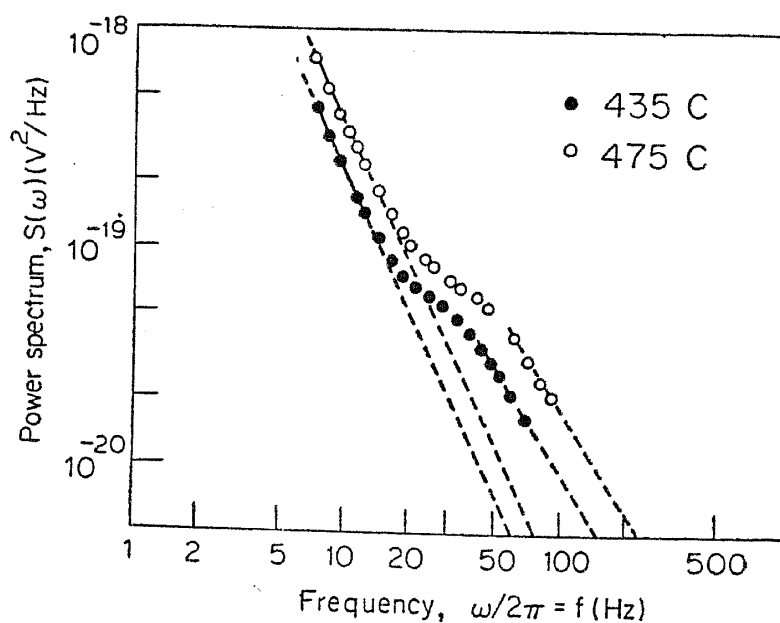$$8\nu \, (I \triangle R)^2 \, \sin^2 \, (\omega\tau/2)/\omega^2, \tag{1}$$

Figure 1. Observed power spectra of the voltage noise in an Al specimen (Celasco *et al* 1976) under constant current conditions. The much larger, but flat, Johnson noise spectrum is eliminated by subtracting out the power spectrum in the absence of a current through the specimen.

where ω denotes the frequency. This expression is now averaged over all positive values of the lifetime τ, with a distribution

$$P(\tau) = (1/\tau_0) \exp(-\tau/\tau_0), \tag{2}$$

about a mean lifetime τ_0. The resultant power spectrum of the voltage noise in a specimen containing an average number N of vacancies is then given by

$$S(\omega) = 4 (I \triangle R)^2 N\nu \, \tau_0^2/(1+\omega^2 \tau_0^2). \tag{3}$$

This is a Lorentzian spectrum. If we further assume, simply, that the average rate of occurrence of pulses is the same as $1/\tau_0$, then

$$S(\omega) = 4 (I \triangle R)^2 N\tau_0/(1+\omega^2 \tau_0^2), \tag{4}$$

the form assumed by CFM in the analysis of their experiment. They obtain, finally the numerical values $\triangle \rho = 1.87$ and $1.85 \, \mu \, \Omega \, \text{cm/at} \, \%$ for the vacancy contribution to the *resistivity** of Al at 435°C and 475°C respectively, with an estimated error of less than 10%. CFM have thus developed an elegant experimental method of measuring the vacancy contribution under *equilibrium* conditions, and at fairly *high* temperatures. Another favourable point is the fact that the measured spectrum depends on the *square* of $\triangle \rho$, allowing for greater precision in the determination of the latter quantity.

We regard the above measurement of the power spectrum resulting from resistivity fluctuations as a very significant development, heralding the feasibility of *resistance fluctuation spectroscopy* (Venkataraman 1975). The experiment vindicates the introduction of correlation methods in yet another class of physical techniques, that of resistivity measurements. In the case chosen by CFM for study, and in several other cases as well, it is the number fluctuations of a specific entity that are responsible for the fluctuations in the resistivity and various other physical quantities. Such entities interact with each other and with other species, diffuse from one point to another, and are absorbed and emitted by sinks and sources such as grain boundaries. In view of the considerable generality of the problem (ranging, for example, from strain fluctuations in crystalline solids to concentration fluctuations in chemical reactions), it is worth analysing the number fluctuations of a species that undergoes both reaction and diffusion in a noisy manner, and which is confined in a *finite* medium. In most cases, much of the information required is contained in the corresponding auto-correlation. It is desirable, therefore, to calculate the power spectrum of number fluctuations in a reactive-diffusive system in a finite geometry. Subsequent application to the experimental results of CFM naturally enables us to dispense with the rather *ad hoc* pulse-sequence type of model (equation (4)) assumed by CFM, and to understand the role played by each relevant physical parameter.

This is the task we have performed in this paper. For the sake of definiteness, we have worked in the framework of the resistivity problem pertinent to CFM, but

---

*$\triangle \rho$ is related to $\triangle R$ by $\triangle \rho = (\triangle R) C_A \, s^2/100$, where C_A is the number of atoms per unit volume and s is the cross-sectional area of the specimen, for the geometry used in CFM.

the formalism may be modified to suit other cases. Our method consists in computing the autocorrelation of the vacancy number density $n(\mathbf{r}, t)$ with the help of a simple stochastic reactive-diffusive equation for that random variable. The 'strengths' of the stochastic sources driving the density fluctuations occur in the answer. These parameters are eliminated in favour of known physical quantities (the diffusion coefficient, average lifetime and equilibrium concentration of vacancies) with the help of a fluctuation-dissipation theorem. The final result is an analytical expression for the power spectrum of the corresponding voltage noise, which is then studied in detail.

We have organised the rest of this paper as follows. In § 2, we set up the problem of evaluating the power spectrum of the voltage noise and the stochastic equation for $n(\mathbf{r}, t)$. An important physical fact is then incorporated in the theory—namely, that the experimental specimen generally has a grain structure, with the grain boundaries acting as the predominant sources and sinks for vacancies. The grains are assumed to be spherical, for simplicity, and the stochastic differential equation for $n(\mathbf{r}, t)$ is solved with appropriate boundary conditions. The autocorrelation of $n(\mathbf{r}, t)$ and thence the power spectrum $S(\omega)$ are calculated exactly, in closed form. The key steps in the calculation are outlined in the Appendices. In § 3, we first consider the special cases corresponding to 'reaction' alone (no diffusion) and to diffusion alone (no reaction: applicable to density fluctuations of, say, interstitial impurity atoms). The different time scales and frequency regimes relevant to the problem are then identified. Three distinct quantities with the dimensions of time occur in $S(\omega)$: the average vacancy lifetime, the 'diffusion time' $\tau_d = l^2/D$ where l is the average grain diameter and D is the diffusion coefficient for monovacancies, and of course ω^{-1}. The interplay of these parameters leads to a spectrum with an interesting structure. In § 4, we compare the theory developed with the (albeit " preliminary ") results of CFM. We find that the high-frequency component that represents the monovacancy contribution is well explained by the form of the power spectrum we have derived; in the frequency range actually covered in the experiment, the spectrum is largely a 'reactive' one (i.e., a Lorentzian as in (4)), but with definitely detectable corrections owing to the occurrence of diffusion in addition. These corrections become more important as the frequency increases. At higher frequencies, just beyond the upper limit ($\sim 10^2$ Hz) of the range covered in CFM, the 'diffusive' contribution is expected to begin to dominate. The power spectrum, however, drops below presently measurable levels. Asymptotically, $S(\omega)$ will reduce to an $\omega^{-3/2}$ power law controlled entirely by the diffusion of vacancies. That this effect is already incipient in the observed power spectrum is clear from the value ($-1\cdot6$) quoted earlier for the slope in the log-log plot of $S(\omega)$ against ω. This value is quite close to the predicted asymptotic value $-1\cdot5$, and is appreciably different from the value -2 expected of a purely Lorentzian spectrum. We also comment in §§ 3 and 4 on the grain-size dependence of $S(\omega)$, a feature which provides a convenient handle for future experiments. An observation is made on the possible nature of the entity responsible for the low-frequency component of the observed power spectrum, by noting the temperature independence of the quantity $S(\omega)/N$, where N is the total number of vacancies in the material under equilibrium conditions at a given T. In § 5, we conclude with some remarks on the applicability and utility of the theory in regard to certain other problems, to be reported elsewhere.

2. Theory

2.1. *Power spectrum of the voltage noise*

As explained in § 1, we hold the vacancy number fluctuations responsible for the voltage noise in the specimen. The predominant sources and sinks for vacancies are the grain boundaries. We assume that the experimental sample is made up of n_g grains of average volume Ω. The boundaries are taken to be perfect sources and sinks for vacancies, with no correlations between different grains. For simplicity, we further assume each grain to be a sphere of radius l, so that $\Omega = 4\pi l^3/3$.

Let $\triangle R$ denote the change in resistance of the specimen due to a single vacancy, as in CFM. If $n_i(\mathbf{r}, t)$ is the instantaneous concentration of vacancies at the point $\mathbf{r}$ in the ith grain at time t, the instantaneous resistance of the sample is

$$R(t) = \triangle R \sum_i \int_\Omega d\mathbf{r}\, n_i(\mathbf{r}, t). \tag{5}$$

We regard $n_i(\mathbf{r}, t)$ as a stochastic variable.* Under steady state conditions, the power spectrum of the voltage noise is obtained from the autocorrelation function

$$\langle V(t_0)V(t_0+t)\rangle_{\text{eq}} = (I\triangle R)^2\, n_g \int_\Omega d\mathbf{r} \int_\Omega d\mathbf{r}'\, \langle n(\mathbf{r}, t_0)n(\mathbf{r}', t_0+t)\rangle_{\text{eq}}. \tag{6}$$

Here $\langle\ \rangle_{\text{eq}}$ stands for the non-transient, i.e., the $t_0 \to \infty$ limit of the correlation function. We have also made use of the lack of correlation between different grains, so that $\mathbf{r}$ and $\mathbf{r}'$ in (6) range over the volume of the same, given grain.

In equilibrium, there is a constant, uniform concentration n_0 of vacancies in the specimen. This number is independent of $\mathbf{r}$ and the grain label i, and depends on the temperature and other physical parameters. Let us write

$$\delta n(\mathbf{r}, t) = n(\mathbf{r}, t) - \langle n(\mathbf{r}, t)\rangle_{\text{eq}} \equiv n(\mathbf{r}, t) - n_0. \tag{7}$$

The power spectrum of the voltage noise is then given by

$$S(\omega) = 4(I\triangle R)^2 n_g \int_\Omega d\mathbf{r} \int_\Omega d\mathbf{r}' \int_0^\infty dt \cos \omega t \cdot \langle \delta n(\mathbf{r}, t_0)\, \delta n(\mathbf{r}', t_0+t)\rangle_{\text{eq}}. \tag{8}$$

The correlation function required will be computed with the help of a stochastic equation for $\delta n(\mathbf{r}, t)$.

2.2. *Reactive-diffusive stochastic equation*

If spatial inhomogeneities are ignored, a simple phenomenological rate equation for the vacancy concentration is $\dot{n} = -\lambda(n - n_0)$, where λ is the inverse of the average

---

*This is a practical, phenomenological approach. The resistance is taken to be proportional to the defect concentration, and fluctuations in the latter are studied. A more formal analysis in terms of 'slow' fluctuations in the dynamical structure factor is possible, and is described elsewhere (Venkataraman and Balakrishnan 1978).

vacancy lifetime. The actual rate of change of the vacancy concentration, however, is an inherently noisy process. Further, the diffusion of vacancies within each grain must be taken into account and this is also a noisy process. The phenomenological rate equation must be replaced, therefore, by the random equation

$$\frac{\partial}{\partial t} n(\mathbf{r}, t) = - \lambda(n(\mathbf{r}, t) - n_0) + f(\mathbf{r}, t) - \nabla \cdot \mathbf{j}(\mathbf{r}, t), \tag{9}$$

where the final term on the right represents the diffusion current into the volume element about the point $\mathbf{r}$. The second term on the right is a stochastic source, the analogue of the random force in the familiar Langevin equation. For the noisy current $\mathbf{j}$, we must again use Fick's law together with another stochastic source:

$$\mathbf{j}(\mathbf{r}, t) = -D\nabla n(\mathbf{r}, t) + \mathbf{g}(\mathbf{r}, t), \tag{10}$$

where D is the diffusion constant for vacancies in a grain. To proceed, we must of course specify the statistical properties of $f(\mathbf{r}, t)$ and $\mathbf{g}(\mathbf{r}, t)$. The simplest theory corresponds to the white noise assumption for these sources*, expressed by

$$\langle f(\mathbf{r}, t) f(\mathbf{r}', t') \rangle = \Gamma_f \, \delta(\mathbf{r} - \mathbf{r}') \, \delta(t - t'),$$

$$\langle g_\alpha(\mathbf{r}, t) g_\beta(\mathbf{r}', t') \rangle = \Gamma_g \, \delta_{\alpha\beta} \, \delta(\mathbf{r} - \mathbf{r}') \, \delta(t - t'), \tag{11}$$

where α, β are Cartesian indices, and further

$$\langle f(\mathbf{r}, t) g_\alpha(\mathbf{r}', t') \rangle = 0. \tag{12}$$

Combining (9)–(12), we obtain the stochastic equation

$$\frac{\partial}{\partial t} \delta n(\mathbf{r}, t) = - \lambda \delta n(\mathbf{r}, t) + D\nabla^2 n(\mathbf{r}, t) + F(\mathbf{r}, t), \tag{13}$$

where the driving term

$$F(\mathbf{r}, t) = f(\mathbf{r}, t) - \nabla \cdot \mathbf{g}(\mathbf{r}, t) \tag{14}$$

is correlated according to

$$\langle F(\mathbf{r}, t) F(\mathbf{r}', t') \rangle = (\Gamma_f + \Gamma_g \nabla_r \cdot \nabla_{r'}) \, \delta(\mathbf{r} - \mathbf{r}') \, \delta(t - t'). \tag{15}$$

Equations (13)–(15) are, of course, precisely the same in form as those which obtain in a linear, one-component reactive-diffusive chemical reaction (Grossmann 1976;

---

*One may, of course, generalize the formalism by a more complicated choice of statistics for f and g. For instance, the 'strengths' Γ_f and Γ_g in (11) may be made dependent on $\mathbf{r}$ and t. Or 'memory' effects may be included by taking f and g to be exponentially correlated sources instead of white noise. These modifications necessitate going over to a generalized (integro-differential) stochastic equation for n, with $\mathbf{r}$- and t-dependent kernels replacing the constants λ and D. However the power spectrum of the voltage has a physically transparent and yet sufficiently rich structure even in our simple model, as we shall see in what follows.

Gardiner 1976). The difference here is merely in the boundary condition, which we write as $\delta n(\mathbf{r}, t)=0$ for $r=l$, corresponding to the fact that the grain boundaries act as perfect sources and sinks for the vacancies. The solution of (13) and evaluation of the correlation function required for the power spectrum in (8) are given in Appendix A.

Using the results obtained there, the power spectrum is found to be

$$S(\omega) = (4/\pi)\, n_g\, (I \triangle R l^3)^2 \int d\mathbf{q}\; [j_1\, (ql)/ql]^2.$$

$$\cdot\, (\Gamma_f + q^2 \Gamma_g)/[(Dq^2 + \lambda)^2 + \omega^2]. \tag{16}$$

Here, j_1 is the spherical Bessel function of order 1, and l is the average radius of a grain, as already mentioned. The integration is over all values of the momentum $\mathbf{q}$. We shall not pause to discuss the form of the above result here, beyond remarking that its structure is very intimately connected with the incorporation of diffusion in a *finite* geometry. A unified discussion is given in § 3. We first eliminate the unknown parameters Γ_f and Γ_g with the aid of the fluctuation-dissipation theorem.

2.3. A fluctuation-dissipation relationship

The driving terms in a stochastic equation such as (13) cause random excursions of the system from its equilibrium state, and fluctuation-dissipation (FD) relationships express the manner in which these fluctuations are damped. Since the equation we are concerned with is comparatively simple, the derivation of these relationships is quite easy, the only noteworthy point being that two independent variables ($\mathbf{r}$ and t) are involved. In Appendix B, the FD theorems pertinent to (13) are written down. We need here the special case of the second FD theorem that is expressed by (B. 5). This reads

$$\Gamma_f + q^2\, \Gamma_g = \Omega\, (Dq^2 + \lambda)\, \langle (\delta n(\mathbf{0}, t_0))^2 \rangle_{\mathrm{eq}}, \tag{17}$$

where (to recall our notation) Ω is the volume of a grain. Of course, no information is obtainable from the stochastic equation for $\delta n(\mathbf{r}, t)$ regarding the mean square or equal-time, same-site correlation involved in the above relation. However, it is physically plausible and quite reasonable to assume that the vacancy number fluctuations are locally Poissonian, i.e., that the variance is equal to the mean at equal times for two points in the same infinitesimal volume element. More rigorous arguments (e.g., using master equation methods—see Gardiner *et al* 1976; van Kampen 1977) support this statement (Gardiner 1976; Grossmann 1976). Expressed mathematically,

$$\langle (\delta n(\mathbf{r}, t_0))^2 \rangle_{\mathrm{eq}} = \langle (\delta n(\mathbf{0}, t_0))^2 \rangle_{\mathrm{eq}} = n_0/\Omega. \tag{18}$$

The FD theorem then becomes

$$\Gamma_f + q^2\, \Gamma_g = n_0(Dq^2 + \lambda). \tag{19}$$

2.4. *Final expression for the power spectrum*

It only remains to substitute (19) in equation (16) for $S(\omega)$. The angular integrals in (16) trivially yield a factor 4π. We may further change the variable of integration to $x=ql$, use $4\pi l^3/3=\Omega$, and also write N for $n_g n_0 \Omega$, the total number of vacancies in the specimen. Finally, it is convenient to introduce the time scale $\tau_d=l^2/D$ associated with the diffusion of a vacancy across a grain. The expression for the relevant correlation function is found to be

$$\int\limits_\Omega dr \int\limits_\Omega dr' \langle \delta n(r, t_0)\delta n(r', t_0+t)\rangle_{eq}$$

$$= (3/\pi)n_0\,\Omega \int\limits_0^\infty dx\, j_1^2(x)\exp[-(x^2+\lambda\tau_d)t/\tau_d],\ (t>0) \tag{20}$$

where $j_1(x) = (\sin x - x\cos x)/x^2.$ \hfill (21)

Substituting this in (8), the required power spectrum is

$$S(\omega) = (12/\pi)(I\triangle R)^2\,N\tau_d \int\limits_0^\infty dx\, j_1^2(x)(x^2+\lambda\tau_d)\cdot[(x^2+\lambda\tau_d)^2+\omega^2\tau_d^2]^{-1}. \tag{22}$$

We note that two characteristic time scales, λ^{-1} and τ_d, occur simultaneously. Their interplay produces an interesting structure for the power spectrum. While a considerable amount of information on this structure can be obtained directly from the integral representation (22), for instance by scaling arguments, we have also been able to evaluate the integral fully in closed form in terms of elementary functions.[*] Our final answer reads

$$S(\omega) = 2(I\triangle R)^2\,N\,[\lambda/(\lambda^2+\omega^2)$$

$$+ \tfrac{3}{2}\,\tau_d\,\mathrm{Re}\,\{z^5-z^3-z^2\,(z+1)^2\exp(-2/z)\}], \tag{23}$$

where $z = [(\lambda+i\omega)\tau_d]^{-1/2}.$ \hfill (24)

3. Discussion

Numerical evaluation and comparison with experiment are given in § 4. Prior to that, it is instructive to study analytically the behaviour of $S(\omega)$ in order to highlight the physical processes involved. We consider, in particular, two limiting cases: the purely reactive one (thus also recovering the result of CFM) and the purely diffusive one, respectively.

---

[*]Unfortunately, there is an error in the value quoted for the basic integral sought in various tables of integrals (e.g., Oberhettinger 1972), and the errata were not available to us. We have therefore indicated the source of the error and evaluated the integral in Appendix C.

3.1. *Purely reactive case: no diffusion*

As already stated in § 1, CFM regard the voltage noise as arising from fluctuations in the lifetime of vacancies. The spatial distribution and movement of vacancies is tacitly assumed to play no role. The power spectrum of CFM is then a simple Lorentzian, as in (4). This is very easily obtained as a special case of our result on letting $D \to 0$, i.e., $\tau_d \to \infty$ in (23). The second term in the square brackets vanishes in this limit, yielding

$$[S(\omega)]_{\text{reac}} = 2(I \triangle R)^2 \, N\tau_0/(1+\omega^2\tau_0^2), \tag{25}$$

where $\tau_0 = \lambda^{-1}$ is the average lifetime of the vacancies. Aside from an overall factor of 2, this is precisely the result of CFM. The explanation for this discrepancy between the two approaches (namely, individual pulses $\triangle R$ of varying duration versus number fluctuations in a stochastic rate equation) has been elaborated upon by Van der Ziel (1953), and will not be repeated here.* In any case, the functional form of the spectrum is not affected; and this form is itself of restricted applicability, being unable to explain the complete structure of the measured spectrum.

There is another circumstance in which the reactive component will dominate, namely, when there are no *finite* boundary effects modulating the diffusion. This case may be studied by letting l (and hence τ_d) become very large, but we should also take into account the corresponding increase in N. The boundary conditions used should also be appropriate to the physical situation. Although we have assumed a spherical geometry in solving the diffusion equation, while the experiment refers to a specimen of length L and rectangular cross-sectional area s, we may make the following comments. Working in terms of intensive quantities, the power spectrum when both L and s become very large can be shown to be

$$S(\omega) \approx \frac{2 \times 10^4 (J\triangle\rho)^2 \eta L}{sC_A} \left[\frac{\lambda}{\lambda^2+\omega^2} - \frac{3b}{2L} \frac{D^{1/2}}{\text{Re}} \, \text{Re} \, (\lambda+i\omega)^{-3/2} + O\left(\frac{1}{L^2}\right) \right]. \tag{26}$$

Here J is the current density, $\triangle\rho$ and C_A have been defined already in § 1, η is the molefraction of vacancies, and b is a numerical factor of the order of unity.

3.2. *Purely diffusive case*

It is of interest to analyse the other extreme case: the effect of the diffusion of infinitely long-lived vacancies in a finite medium. The result obtained in this instance is relevant to other problems as well. For instance, if instead of vacancies, we considered the diffusion of a given number of interstitial impurity atoms dispersed uniformly in the specimen (e.g., hydrogen in Nb, Pd, etc.), the functional form of the power spectrum of the corresponding voltage noise would be similar to the one quoted below.** A measurement of the power spectrum, or, quite conveniently, its leading

---

*The factor is related to the averaging over lifetimes in the pulse sequence approach taken by CFM. The ad hoc exponential distribution (2) produces the extra factor.

**This is not strictly correct. For a given total number of interstitials, we should solve the diffusion equation with somewhat different boundary conditions than the one used in the present paper: the gradient of $n(\mathbf{r}, t)$ normal to the surfaces of the material should be taken to vanish at the boundaries.

high-frequency behaviour, could then provide an accurate determination of the corresponding diffusion coefficient. With some modifications, one can envisage application to other contributions to resistivity fluctuations, such as that due to the diffusion of kinks on dislocations.

The formula desired is obtained by simply taking the limit $\lambda \to 0$ in (23). It is convenient to express the answer as a function of the parameter $\alpha = (2\omega\tau_d)^{1/2}$. We obtain

$$[S(\omega)]_{\text{diff}} = 6 \, (I \triangle R)^2 N\tau_d \, \alpha^{-3} \, [1 + e^{-\alpha} \, (\cos \alpha + \sin \alpha) + 4\alpha^{-1} \, e^{-\alpha} \cos \alpha$$

$$- 2\alpha^{-2} + 2\alpha^{-2} \, e^{-\alpha} \, (\cos \alpha - \sin \alpha)]. \tag{27}$$

The trignometric functions are of course a consequence of our spherical approximation for the grain geometry. The leading asymptotic ($\omega\tau_d \gg 1$) behaviour of the power spectrum is given by

$$[S(\omega)]_{\text{diff}} \approx (3/\sqrt{2}) \, (I \triangle R)^2 \, ND^{1/2} \, l^{-1} \, \omega^{-3/2} + O \, (\omega^{-2}). \tag{28}$$

This ($-3/2$) power dependence on ω is quite expected in a standard diffusion process. At low frequencies, $S(\omega)$ can be expanded in a power series in α, the first two terms of which yield

$$[S(\omega)]_{\text{diff}} \approx \tfrac{4}{5} \, (I \triangle R)^2 \, (Nl^2/D) \, [1 - \tfrac{5}{12} \, (2\omega L^2/D)^{1/2} + \ldots] \tag{29}$$

A remark on the grain size dependence may be made at this stage. We have assumed throughout that all the grains are equal in size, with a common radius l. On the other hand, it is evident that a distribution of sizes and shapes would obtain in an actual experimental specimen. Both these distributions depend on the mode of preparation and the metallurgical history of the sample (Chadwick 1972). A common assumption for the grain size distribution is a narrow Gaussian, little distinguished from the δ-function distribution implicit in the foregoing. An alternate distribution that is also physically realistic is

$$P \, (l) = (l/l_0^2) \exp \, (-l/l_0), \tag{30}$$

with a most probable value l_0 and a mean value $2l_0$. If we average the expressions in (28) and (29) over this distribution, it is easy to see that the power dependence of the results on l_0 is the same as the original l- dependence. Thus the high-frequency power spectrum is proportional to the inverse of the average grain diameter, while the low frequency limit is proportional to its square. The first part of this statement remains true even in the presence of the reactive contribution. So does the latter part, provided $\lambda l_0^2/D \ll 1$ (see (33) below). Precision experiments that measure $S(\omega)$ could thus yield independent values for l_0 if the diffusion constant is known from other sources.

3.3. *Frequency regimes in* $S(\omega)$

Let us first obtain an asymptotic form for $S \, (\omega)$ when $|z| \ll 1$, i.e., when *either*

$\omega \tau_d \gg 1$, *or* $\lambda \tau_d \gg 1$, or *both*. The exponential term in (23) then drops out of the asymptotic expansion, leaving behind

$$S(\omega) \approx 2 (I \triangle R)^2 N [\lambda/(\lambda^2 + \omega^2) + \tfrac{3}{2} \tau_d \, \mathrm{Re}\, (z^5 - z^3)], \tag{31}$$

where z has been defined in (24). If now $\omega \gg \lambda$, the leading behaviour is purely diffusion-controlled, and is given by

$$S(\omega) \approx (3/\sqrt{2})(I \triangle R)^2 N (\omega \tau_d)^{-3/2}, \tag{32}$$

which is precisely the result (28). The comments made following (29) apply here too. At somewhat lower frequencies, provided λ continues to remain much larger than $1/\tau_d$, (31) provides a convenient representation for the power spectrum, corrections to the expression being of order

$$\exp\,[-\tau_d \,(\lambda^2 + \omega^2)^{1/2}].$$

At the other end of the spectrum, we have $|z| \gg 1$, which implies that $\omega \tau_d \ll 1$ *and* $\lambda \tau_d \ll 1$, without the *relative* magnitudes of ω and λ being specified. We find then

$$S(\omega) \approx \frac{4}{5}(I \triangle R)^2 N \tau_d \left[1 - \frac{5}{6}\left(\frac{\tau_d}{2}\right)^{1/2}((\lambda^2 + \omega^2)^{1/2} + \lambda)^{1/2} + \frac{3}{7}\lambda \tau_d + \ldots\right]. \tag{33}$$

When $\lambda = 0$, this matches equation (29) of the purely diffusive case. If $\omega \ll \lambda$, the power spectrum to leading order in ω is given by

$$S(\omega) \approx \frac{4}{5}(I \triangle R)^2 N \tau_d \left[1 - \frac{5}{6}(\lambda \tau_d)^{1/2} + \frac{3}{7}\lambda \tau_d - \frac{5}{48}(\lambda \tau_d)^{1/2}\frac{\omega^2}{\lambda^2}\right]. \tag{34}$$

4. Comparison with experiment

Although the results quoted by CFM are of " a preliminary nature ", it is instructive to compare experiment with theory. The data of CFM are shown in figure 1. Error bars have not been shown, for clarity. To recall the statement made in § 1, $S(\omega)$ exhibits two distinct regimes, in each of which it is roughly consistent with a pure power law of the type $S \sim \omega^{-\gamma}$, i.e., a straight line in the log-log plot with a slope equal to $-\gamma$. Such a power law behaviour is already current at the beginning of the experimental frequency range, namely, $\omega/2\pi = f \approx 7$ Hz. The average value of the exponent γ is found to be 2·07 at $T = 435°C$ and 2·00 at $T = 475°C$. The high frequency regime $(f \gtrsim 40)$ is again consistent with a linear log-log plot. It is significant that the slope is now smaller in magnitude, the average values of the exponent working out to be 1·64 and 1·60 respectively at 435°C and 475°C. We attach considerable importance to this fact.

We state at the outset that our theory does not explain the component that is dominant at the low frequency end. This will become clear as we proceed, but a glance at figures 2 through 4 makes this evident. It appears that the monovacancy
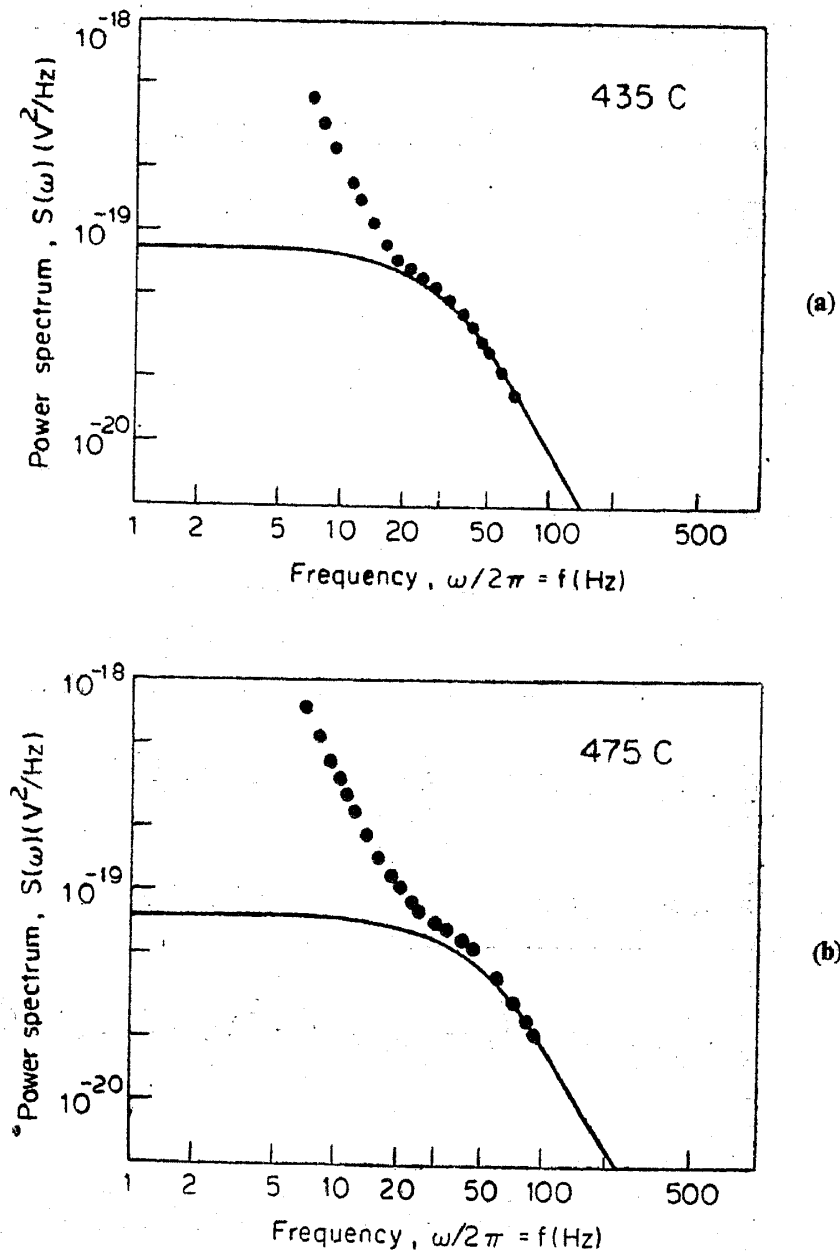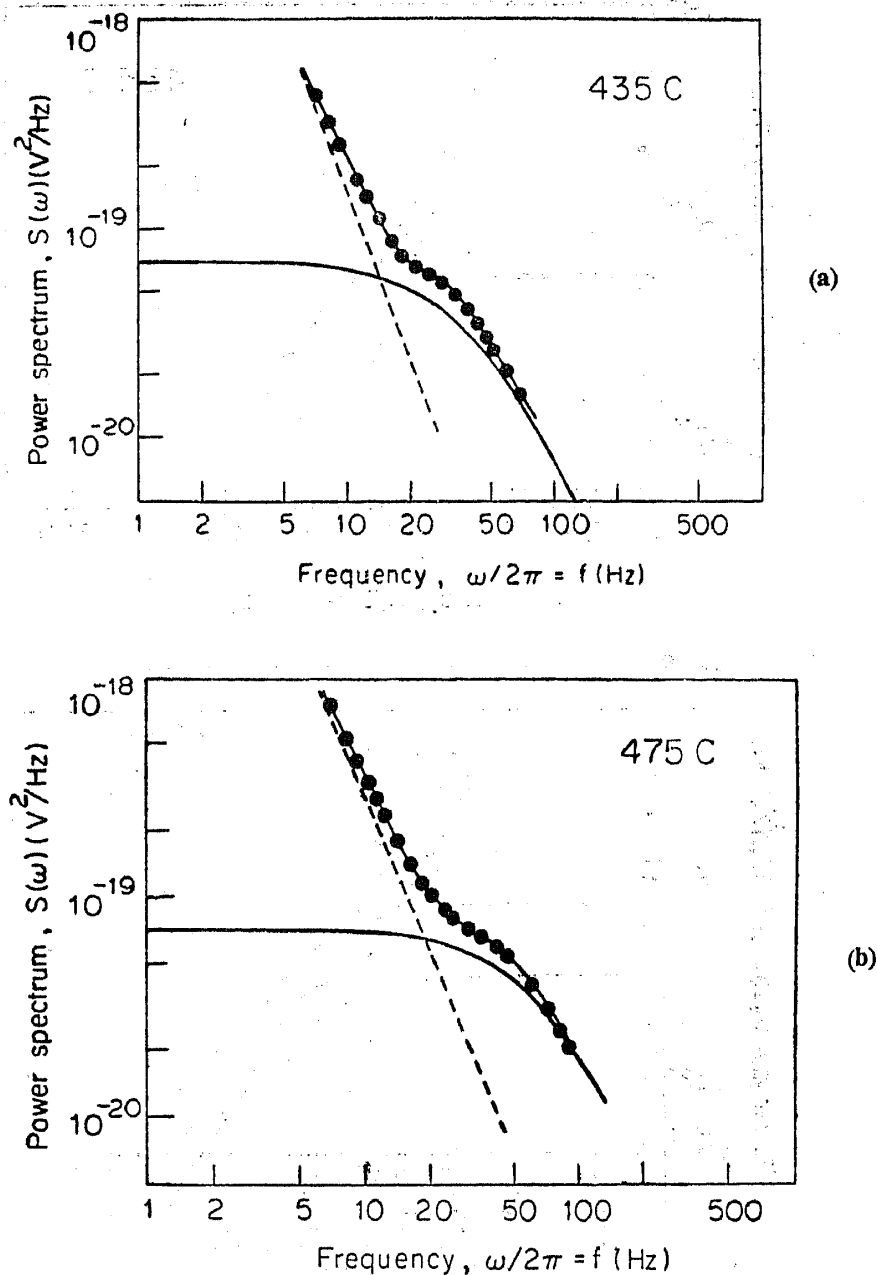
Figure 2. Fits to the observed spectra from theory (equation (31)), regarding both τ_d and $(I\Delta R)^2 N$ as adjustable parameters, to illustrate the functional form of the calculated expression. Note that the low-frequency component is neglected in these fits for the high-frequency component.

contribution we have been concerned with is largely responsible for the observed power spectrum beyond $f \approx 40$ Hz. At low frequencies ($\lesssim 15$ Hz) this contribution tends to a constant value that is roughly an order of magnitude smaller than the observed power spectrum at the lowest experimental frequencies, $f \approx 7$ Hz. There exists, therefore, some other mechanism whose contribution reaches asymptopia, i.e., which is effectively of the form $S \sim \omega^{-\delta}$, already at $f \approx 7$ Hz. We shall deduce an approximate value for δ by subtracting the vacancy contribution from the measured power spectrum.

Before we can fit the high-frequency component of the observed spectrum to the theoretical expression derived, it is necessary to know the values of the parameters

Figure 3. Fits (continuous lines) assuming a purely Lorentzian spectrum, i.e., diffusive effects being neglected. These fits are essentially unaltered when diffusive effects are included, but when the average grain diameter is taken to be ≈ 25 μm, i.e., a single grain assumption for the specimen used by CFM. The fits are unsatisfactory (see text); note the intersection with the observed spectrum in figure 3b.

occurring in (23), namely, λ, τ_d and $(I \triangle R)^2 N$. It has already been pointed out that CFM have assumed a Lorentzian type of spectrum for the high-frequency component, and deduced a value for $\triangle R$ from the data. We find, on the other hand, that the spectrum as given by (23) has a diffusion contribution as well. The values of λ, the inverse of the average vacancy lifetime, as quoted in CFM are 214 sec^{-1} (at 435°C) and 357 sec^{-1} (at 475°C). We do not have a value for $\tau_d = l^2/D$, as the average grain size in the experimental samples of CFM is not available. However, this is certainly greater than 1 μm. The monovacancy diffusion constant in Al may be calculated
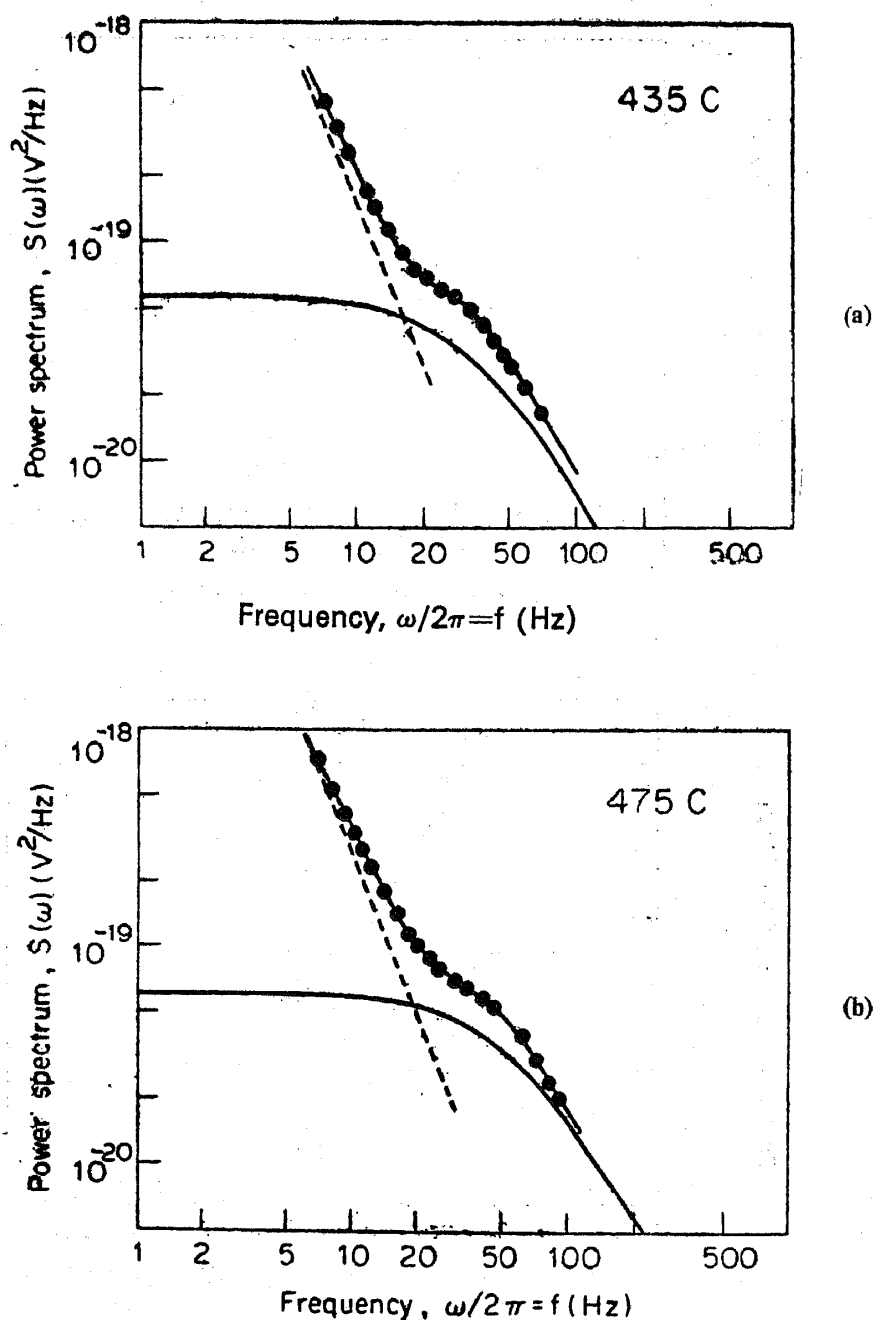
Figure 4. Theory *vs* experiment: the continuous lines represent the vacancy contribution to the power spectra as evaluated in the present work. Subtraction from the measured spectra yields the low-frequency component (dashed lines), presumably caused by vacancy clusters.

from the numbers quoted in Seeger and Mehrer (1970). We find $D = 2.33 \times 10^{-7}$ cm^2 sec^{-1} and 4.02×10^{-7} cm^2 sec^{-1} respectively at 435°C and 475°C. Thus τ_d is certainly larger than 0.1 sec, so that $\lambda \tau_d$ exceeds unity by a considerable amount. One may therefore drop the exponential term in (23) and work with the formula (31), in the present instance.

Suppose we treat $(I \triangle R)^2 N$ and τ_d as *adjustable* parameters, and use them in (31) to fit (the high-frequency component of) the spectrum. Typical results are shown in figures 2a and 2b, which are meant to *illustrate* the functional form of the

theoretical spectrum. At the low frequency end, $S(\omega)$ as given by (31) saturates to the value

$$S(o) = 2(I\triangle R)^2(N/\lambda) \left[1 - \frac{3}{2(\lambda\tau_d)^{1/2}} \left(1 - \frac{1}{\lambda\tau_d} \right) \right].$$ (35)

At higher frequencies, the diffusive contribution provides a correction to the reactive or Lorentzian contribution. As f increases beyond $\lambda/2\pi$ (34 Hz at 435°C and 57 Hz at 475°C), this correction is no longer negligible. The dependence of S on the parameters concerned is brought out somewhat more clearly if we rewrite (31) in the form

$$S(\omega) = (I\triangle R)^2 N \left[\frac{2\lambda}{\Lambda^2} - \frac{3}{(\Lambda\tau_d)^{3/2}} \left\{ \tau_d \cos 3\theta - \frac{1}{\Lambda} \cos 5\theta \right\} \right],$$ (36)

where $\Lambda = (\lambda^2 + \omega^2)^{1/2}$, (37)

and $\theta = \tan^{-1} [(\Lambda-\lambda)/(\Lambda+\lambda)]$. (38)

As $f = \omega/2\pi$ runs from 0 to ∞, θ increases from 0 to $\pi/4$. At some point beyond $\theta = \pi/6$ ($f \approx 120$ Hz for 435°C and 200 Hz for 475°C), the effect of diffusion begins to dominate, till finally the power spectrum is essentially given by the $\omega^{-3/2}$ power law of (32). The experimental range of frequencies for which numerical values are reported by CFM does not extend to this asymptotic region. However, the observed spectrum beyond $f \approx 40$ Hz is not a pure Lorentzian (as assumed by CFM), and does exhibit the effects of the term involving τ_d in (36), as we shall see. This is already manifest in the fact that $S(\omega)$ varies roughly according to a power law with exponent $\approx -1\cdot6$ at the upper end of the experimental frequency range.

We have already said that the fits shown in figures 2a and 2b merely serve as illustrations. In particular, these fits ignore the low-frequency component of the observed spectra, in the sense that this component has been essentially assumed to be zero and only the high-frequency fitted. In reality, the observed spectrum is a superposition of the component which dominates at low frequencies (and which is not encompassed by our theory), and that which is given by the theory developed (and which dominates at higher frequencies). We may determine the value of the overall factor $(I\triangle R)^2 N$ appropriate to each temperature by working backwards from the result quoted in CFM for the change in resistivity due to the vacancies, together with the values given for the current density and the dimensions of the experimental specimen. If $\triangle\rho$ is the resistivity change per unit vacancy concentration in atomic per cent, and η is the molefraction of vacancies, CFM find that

$$(\triangle\rho)^2\eta = \begin{cases} 1\cdot3 \times 10^{-16} \ (\Omega \ \mathrm{cm/at\%})^2 & (T{=}435°C) \\ 2\cdot3 \times 10^{-16} \ (\Omega \ \mathrm{cm/at\%})^2 & (T{=}475°C). \end{cases}$$ (39)

We deduce from these values that

$$(I\triangle R)^2 N = \begin{cases} 3\cdot73 \times 10^{-18} \ V^2 & (T{=}435°C) \\ 6\cdot60 \times 10^{-18} \ V^2 & (T{=}475°C). \end{cases}$$ (40)

As a check, we note that the logarithm of the ratio $N(475°C)/N(435°C)$ computed from (40) yields a value 0·65 eV for the monovacancy formation energy E_f, in good agreement with the number 0·66 eV of Seeger and Mehrer (1970). With (40) in hand, T_d remains the only undetermined parameter. Although we do not know l, the average grain diameter in the sample, we can set limits on its magnitude. The experimental specimen used by CFM was a film of dimensions 1·5 μm × 15 μm × 3mm, obtained by a photoetching technique. Suppose we assume that the entire volume of the sample is a single grain. (We have worked with a spherical geometry for the sake of simplicity.) The effective dimension l works out then to be roughly 25 μm. Using the values of D already mentioned, we obtain τ_d=27·3 sec at 435°C and 15·9 sec at 475°C. These values are so large that the diffusive correction to the Lorentzian spectrum is essentially negligible. What happens physically is that the finite mean lifetime of the vacancies is the only effective source of fluctuations in their number at the frequencies of interest. The disappearance of vacancies by diffusion to the boundaries does not contribute comparably. In figures 3a and 3b the continuous solid lines depict the calculated power spectra corresponding to the above-mentioned values of τ_d and with $(I\triangle R)^2 N$ as in (40). The dashed line in each figure represents the 'other' component, obtained by subtracting the calculated power spectrum from the experimental spectrum of CFM. It may be added that, to within the accuracies involved, these same figures *also* represent a fitting of the spectra with Lorentzians *alone* (dropping the term in curly brackets in (36)), as in CFM, for reasons already stated. It may appear that the agreement is reasonable. We claim, however, that this is not so—implying, therefore, that the diffusive corrections to the Lorentzian do affect the spectrum even at the frequencies concerned, and that the true values of τ_d must be somewhat smaller than those used in these fits: The calculated spectrum at T=475°C is too large in magnitude at the high-frequency end, as is immediately clear from figure 3b. While it may seem that there is no manifest discrepancy of this sort in the spectrum corresponding to 435°C, this fit is just as unsatisfactory. For instance, the magnitude of the slope of the calculated spectrum is approximately equal to 1·8 when it reaches rough linearity (in the log-log plot) beyond f=100 Hz; in contrast to this, the observed spectrum reaches linearity already by $f \approx$ 50 Hz, with a slope of magnitude $\approx$ 1·6.

The conclusion, therefore, is that the observed spectrum corresponds to a Lorentzian with significant corrections due to the diffusive effects. We attempt to find an *estimate* for τ_d as follows. Taking a cue from the approximate power law behaviour of $S(\omega)$ at the upper end of the experimental frequency range, with an exponent $\approx$ 1·6 that is not far removed from the asymptotic value 1·5, let us insert the value of S at the highest frequency used in the *asymptotic* formula (32), and solve for τ_d. We find then

$$\tau_d \approx \begin{cases} 0·23 \text{ sec } (T=435°C) \\ 0·21 \text{ sec } (T=475°C). \end{cases} \tag{41}$$

The corresponding power spectra are drawn in figures 4a and 4b. The slope beyond f=100Hz is found from these graphs to be $\approx$ 1·54 at 435°C and $\approx$ 1·50 at 475°C. The average grain diameter now works out to be $\approx$ 2·3 μm at T=435°C and increases to $\approx$ 2·9 μm at 475°C. The actual value is most likely to be somewhat larger, but

certainly less than the 25 μm upper limit.[*] To deduce this value more precisely from a measurement of $S(\omega)$, one either needs a theory for the low-frequency component, or else one must further improve the already impressive sensitivity of the experimental set-up to measure $S(\omega)$ at frequencies beyond 100 Hz. Even data upto just 200 Hz would be most helpful in the present instance.

Finally, regarding the ' other ' component that dominates at low frequencies, we have little to add to the comments made in CFM. The dotted lines in figures 4a and 4b show the variation of this component with frequency. This is approximately a power behaviour of the form $\omega^{-\delta}$, where $\delta = 2.4$ in both cases. It has already been stated that this component is not *directly* related to the monovacancy contribution. However, we have the following interesting observation to make. Let us divide out the measured values of the power spectrum at each temperature by the corresponding overall factor $(I\triangle R)^2 N$ given in (40). The variation of the quantity $S(\omega)/(I\triangle R)^2 N$ with frequency is shown in figure 5. It is evident that the high-frequency component (the monovacancy contribution) that we have been concerned with does exhibit a further temperature dependence, owing to that of λ and τ_d. On the other hand, the low-frequency component is now practically *independent* of T. Thus, whatever be the nature of the entities (e.g., vacancy *clusters*) responsible for this contribution to the power spectrum, the T-dependence of this component arises primarily from that of N, the total number of *monovacancies* in the sample. A plausible picture, therefore, is the following. The low-frequency component is caused by entities other than monovacancies, and already at $f \approx 7$ Hz it has reached a pure power-law behaviour. It is therefore of the form

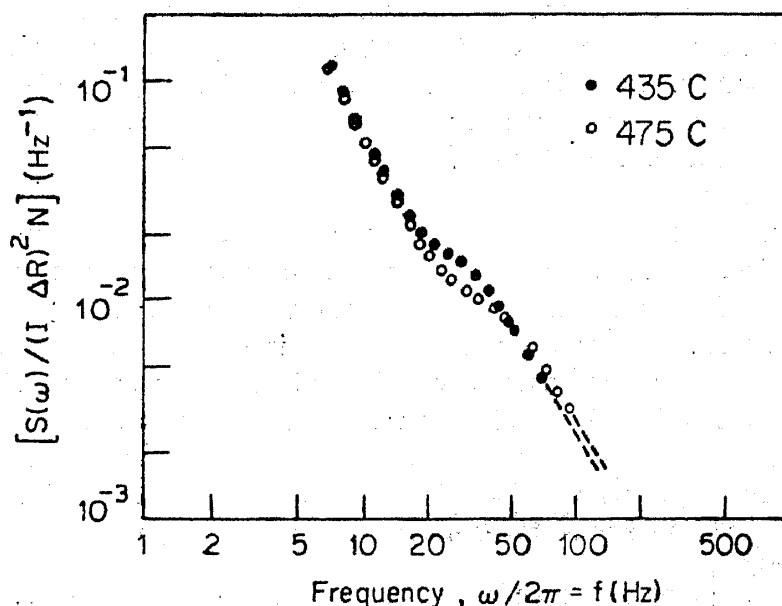$$S(\omega) \sim (I\triangle R')^2 N' \lambda'/\omega^\delta \tag{42}$$

Figure 5. Observed power spectra after scaling out by the overall factor $(I\triangle R)^2/N$. Note the approximate temperature independence of the low-frequency component.

---

[*]A grain whose linear dimensions are of the order of a few microns is still sufficiently large ($>10^4$ atomic distances in each direction) to enable us to use the continuum approximation implied by the diffusion equation.

where $\triangle R'$ is the analogue of the single-vacancy contribution $\triangle R$. The rate equations for the densities $n(\mathbf{r}, t)$ and $n'(\mathbf{r}, t)$ must be coupled to each other. In equilibrium, the total numbers N and N' must be proportional to each other. Further, the effective rate constant λ' for the unknown entities must be only very weakly T-dependent, at least to the extent of being roughly constant as T changes from 435°C to 475°C: hence the observed T-independence of $S(\omega)/N$ at low frequencies. The exponent δ would normally be expected to be equal to 2, if (42) were simply the high-frequency limit of a Lorentzian. The approximate value 2·4 that we have deduced from the data may be the result of correlations (Mazzetti 1964), or, in another language, memory effects—recall that we have assumed white noise stochastic sources in the rate equation for $n(\mathbf{r}, t)$. Finally, the fact that the component in question is already linear at $f \approx 7$ Hz in a log-log plot suggests that $\tau' > 10^{-2}$ sec, where τ' is the mean lifetime of the entities concerned.

5. Concluding remarks

The reactive-diffusive model for number fluctuations that we have developed brings out the existence of the two time scales $1/\lambda$ and τ_d controlling lifetime effects and diffusion respectively. The latter introduces finite geometry effects via l, the average grain diameter. The dependance on l provides *a convenient experimental method* of altering τ_d, with its attendant consequences, as opposed to achieving this by varying the temperature (and hence the diffusion coefficient); besides, varying T also changes the total number N and the lifetime $1/\lambda$, whereas τ_d alone is altered if l is varied.

Our theory is quite general, and several other applications can be envisaged (Venkataraman 1978). It appears to be quite feasible, and very useful, to carry out ' resistance fluctuation spectroscopy ' at the various annealing stages in the recovery of irradiated metals. An advantageous alternative to the conventional method of monitoring the resistivity is thus provided, because one can work directly at the annealing temperature at each stage. Moreover, the technique is likely to yield additional information of importance. For example, one can visualise an independent and fairly direct method of discriminating between alternative pictures of the recovery stages. Ambiguities in reconstructing the sequence of processes that occur physically can therefore be resolved. A much-discussed question (Seeger 1975; Buck and Seeger 1977; Schilling 1975, 1977; Wichert *et al* 1978) is the following: in stage III, do vacancies migrate freely and annihilate at interstitial clusters, or is it single interstitials that migrate and annihilate, having survived till this stage in metastable forms? We believe that the power spectra of the resistance fluctuations in the two schemes will be quite different, because of the dependence on different effective lifetimes and diffusion coefficients, among other reasons, enabling experiment to distinguish between them.

Another conceivable application concerns the behaviour of hydrogen interstitials in metals. In particular, the technique could be used as an aid in the spinodal decomposition in coherent metal-hydrogen systems (Janssen 1976). However, an important and non-trivial generalisation of our theory is needed before this problem is considered. Since the long-range elastic interaction between interstitial H atoms is primarily responsible for their condensation into various phases, the corresponding

stochastic equation for $n(\mathbf{r}, t)$ must include the effects of this interaction. In addition to becoming a non-local integro-differential equation as a consequence, it also becomes a non-linear one, posing considerable difficulties in the way of its solution. Similarly, application to most chemical reactions would also require an extension of our theory to the non-linear regime, for the rate equations governing the deterministic evolution of the average concentrations are themselves essentially non-linear equations or coupled sets of such equations. However, it is possible to develop approximation schemes for the evaluation of the required correlation function (Haken 1977). These equations are of current interest in the study of dynamical critical phenomena, chemical reactions, etc. (Haken 1977; Prigogine and Nicolis 1977; Dewel *et al* 1977).

There are further applications in the field of mechanical properties as well. At sufficiently high values of T/T_M, the diffusion of vacancies in a metal contributes significantly to its plastic deformation under an applied stress. Various forms of such diffusion creep occur (e.g., see Gittus 1975), involving different mechanisms: Nabarro-Herring creep, Coble creep, Harper-Dorn creep. The corresponding creep rates have different grain-size dependences. A careful theoretical analysis of the entire phenomenon involving the simultaneous operation of the various mechanisms, that goes beyond the simple diffusion equation model, is called for (Rama Rao 1978). Here, too, a study of the density fluctuations via an appropriate power spectrum may provide an accurate and convenient method for deducing the time evolution of the average strain, once the two are connected by a fluctuation-dissipation relation. Experimentally too, such a procedure would be considerably faster than the conventional direct monitoring of the creep. It is worth mentioning that this particular application involves non-equilibrium conditions—plastic flow under an applied stress. The *transient* region in time (which was not of interest in the problem considered in this paper) now becomes relevant, and transient terms in the solution for $n(\mathbf{r}, t)$ must be retained. Stationarity does not obtain any longer, and one must identify time scales in which the random processes concerned are quasi-stationary, and work with power spectra appropriate to such processes.

Acknowledgements

Appendix A

Solution for $\delta n(\mathbf{r}, t)$ and its autocorrelation

Equation (13) for $\delta n(\mathbf{r}, t)$, together with the boundary condition $\delta n(\mathbf{r}, t) = 0$ for $r = l$, can be solved by a Fourier transform with respect to $\mathbf{r}$ and a Laplace transform with respect to t, i.e.,

$$\delta n(\mathbf{r}, t) = \frac{1}{2\pi i} \frac{1}{(2\pi)^3} \int_{-i\infty}^{i\infty} dp \int d\mathbf{q} \; \delta\tilde{n}(\mathbf{q}, p) \exp(i\mathbf{q}\cdot\mathbf{r}+pt). \qquad (A.1)$$

Then the non-transient part of $\delta n(\mathbf{r}, t)$ is obtained by substituting the solution

$$\delta\tilde{n}(\mathbf{q}, p) = \tilde{F}(\mathbf{q}, p)/(Dq^2+\lambda+p) \qquad (A.2)$$

in (A.1).   The transient term will give a contribution $\sim \exp(-\lambda t - Dq^2 t)$ to $\delta n(\mathbf{r}, t)$, and is irrelevant for our present purposes.

When this solution is used to compute the correlation function

$$\int_\Omega d\mathbf{r} \int_\Omega d\mathbf{r}' \; \langle \delta n(\mathbf{r}, t_0) \, \delta n(\mathbf{r}', t_0+t)\rangle_{\mathrm{eq}}, \qquad (A.3)$$

we encounter the integral

$$\int_\Omega d\mathbf{r} \exp(i\mathbf{q}\cdot\mathbf{r}) = 3\,\Omega\, j_1(ql)/ql \qquad (A.4)$$

where $j_1(x) = (2/\pi x)^{1/2} J_{3/2}(x) = (\sin x - x \cos x)/x^2.$ \qquad (A.5)

This leads to all the important finite geometry effects discussed in the paper.   We note that in the limit $l \to \infty$, we simply obtain $(2\pi)^3 \delta(\mathbf{q})$ for the value of the integral.

The correlation function (A.3) involves the force autocorrelation

$$\langle \tilde{F}(\mathbf{q}, p) \, \tilde{F}(\mathbf{q}', p')\rangle \qquad (A.6)$$

which can be evaluated with the help of equation (15) for the autocorrelation of $F(\mathbf{r}, t)$.   Carrying out the algebra yields

$$\langle \tilde{F}(\mathbf{q}, p) \, \tilde{F}(\mathbf{q}', p')\rangle = (2\pi)^3 \, (\Gamma_f + q^2\Gamma_s) \, \delta(\mathbf{q}+\mathbf{q}')/(p+p'). \qquad (A.7)$$

The required correlation function entails inversion of the transforms with respect to $\mathbf{q}$, $\mathbf{q}'$, p and p'.   The integration over $\mathbf{q}'$ is trivial because of the presence of the δ-function in (A.7).   We then integrate with respect to p and p', and drop a transient term proportional to $\exp[-(Dq^2+\lambda(2t_0+t)]$.   Again, we omit the algebra and quote the result:

$$\int_\Omega d\mathbf{r} \int_\Omega d\mathbf{r}' \; \langle \delta n(\mathbf{r}, t_0) \, \delta n(\mathbf{r}', t_0+t)\rangle_{\mathrm{eq}} = (l^6/\pi) \int d\mathbf{q} \; [j_1(ql)/ql]^2.$$

$$\cdot \, [(\Gamma_f + q^2\Gamma_s)/(Dq^2 + \lambda)] \exp[-(Dq^2 + \lambda)t], \; (t > 0) \qquad (A.8)$$

Integrating this with respect to t from 0 to ∞ with the factor $\cos \omega t$ in accordance with (8) yields the desired power spectrum.   This is written down in (16).

Appendix B

The fluctuation-dissipation theorems

While we need only a special case of the *second* FD theorem in the text (eq. (17)), it is not difficult to derive the general forms of the first and second FD theorems (Kubo 1966) pertinent to the reactive-diffusive stochastic eq. (13). The procedure is similar to the one used (Balakrishnan 1976) in the case of the generalised Langevin equation, and is indeed simpler because of the white noise nature of $F(\mathbf{r}, t)$. The only minor complication is the spatial dependence of the variables. We shall merely quote our results here.

We find that the first FD theorem in the present situation reads

$$\int_0^\infty dt \ \langle \delta n(\mathbf{q}, t_0) \ \delta n(\mathbf{q}', t_0 + t) \rangle_{\text{eq}} = \frac{\langle \delta n(\mathbf{q}, t_0) \ \delta n(\mathbf{q}', t_0) \rangle_{\text{eq}}}{(Dq'^2 + \lambda)}. \qquad (B.1)$$

Here $\delta n(\mathbf{q}, t)$ denotes the spatial Fourier transform of $\delta n(\mathbf{r}, t)$ and $\langle\ \rangle_{\text{eq}}$ refers to the stationary (or $t_0 \to \infty$) regime. This theorem relates the autocorrelation of δn to its mean squared value in equilibrium.

The second FD theorem involves the autocorrelation of the random source, and turns out to be

$$\langle \delta n(\mathbf{q}, t_0) \ \delta n(\mathbf{q}', t_0) \rangle_{\text{eq}} = (2\pi)^3 \ \delta(\mathbf{q}+\mathbf{q}') \ (\Gamma_f + q'^2 \Gamma_g)/(Dq'^2 + \lambda). \qquad (B.2)$$

This is the generalization of a more restrictive relation, which is

$$\langle \delta n(\mathbf{q}, t_0) \delta n(-\mathbf{q}, t_0) \rangle_{\text{eq}} = \Omega \ (\Gamma_f + q^2 \Gamma_g)/(Dq^2 + \lambda). \qquad (B.3)$$

We may revert to co-ordinate space on the left-hand side, and use the fact that, at *equal* times,

$$\langle \delta n(\mathbf{r}, t_0) \ \delta n(\mathbf{r}', t_0) \rangle_{\text{eq}} = \Omega \ \langle (\delta n(\mathbf{r}, t_0))^2 \rangle_{\text{eq}} \ \delta(\mathbf{r}-\mathbf{r}'). \qquad (B.4)$$

Equation (B.3) then yields

$$\Gamma_f + q^2 \Gamma_g = \Omega \ (Dq^2 + \lambda) \ \langle (\delta n(0, t_0))^2 \rangle_{\text{eq}}, \qquad (B.5)$$

and this is the theorem used in the text in § 2.3.

Appendix C

Evaluation of the integral for $S(\omega)$

We start with equation (22) for $S(\omega)$. Breaking up the denominator in the integrand into partial fractions, we get

$$S(\omega) = 6(I \triangle R)^2 N \tau_d \int_0^\infty dx \ x^{-1} J_{3/2}^2 (x). \ \text{Re} \ [x^2 + (\lambda + i\omega)\tau_d]^{-1}. \qquad (C.1)$$

We have then merely to find the value of the integral

$$\int_0^\infty dx\; x^{-1}\,(x^2+k^2)^{-1}\,J_{3/2}^2\,(x),\quad \mathrm{Re}\;k>0,\tag{C.2}$$

in order to solve our problem. It is easily seen that the integral converges, even for $k=0$. Unfortunately an incorrect value (reducing to a negative definite quantity when k is a positive number) is quoted in various standard tables; hence this Appendix. Our procedure may be used to correct the values of various associated integrals listed in the tables, as well.

Instead of (C.2), let us begin with the integral (Watson 1928)

$$\mathcal{J}(\mu) = \int_0^\infty dx\; x^{\mu-1}\,(x^2+k^2)^{-1}\,J_{3/2}\,(x)\,H_{3/2}^{(1)}\,(x)\tag{C.3}$$

where $0<\mathrm{Re}\;\mu<3$ and $H_{3/2}^{(1)}$ is the Hankel function of the first kind. The integral can be evaluated by considering a contour running just *above* the real axis from $-\infty$ to $+\infty$ (both the Bessel functions have branch cuts from $-\infty$ to 0) and closing it with a large semicircle in the upper half plane—hence the introduction of $H_{3/2}^{(1)}$. Convergence at the origin, vitiated by $H_{3/2}^{(1)}$, is restored by the introduction of x^μ with $\mathrm{Re}\;\mu>0$. Cauchy's theorem may be applied to pick up the contribution of the pole at $x=+ik$ where k stands for the square root of k^2 with $\mathrm{Re}\;k>0$. In the integral above the negative real axis, we use the relations

$$J_{3/2}\,(x\,\exp\,(i\pi)) = \exp\,(3i\pi/2)\,J_{3/2}\,(x),$$

$$H_{3/2}^{(1)}\,(x\,\exp\,(i\pi)) = \exp\,(-3i\pi/2)\,[H_{3/2}^{(1)}\,(x) - 2\,J_{3/2}\,(x)].\tag{C.4}$$

On analytic continuation to $\mu=0$, the $J_{3/2}\,H_{3/2}^{(1)}$ terms cancel out, leaving behind on the left-hand side essentially the integral in (C.2), together with a contribution from a small semicircle of radius ϵ around the origin in the upper half plane. The latter is non-zero for the simple reason that

$$\lim_{\epsilon\to0}\;\lim_{\mu\to0}\;\epsilon^\mu = 1\;(\neq0),\tag{C.5}$$

and the omission of this contribution is responsible for the error referred to above. Using the definition $H_{3/2}^{(1)} = J_{3/2}+iN_{3/2}$ together with the leading behaviour

$$J_{3/2}\,(z) \sim z^{3/2},\quad N_{3/2}\,(z) \sim z^{-3/2}\tag{C.6}$$

for $z \to 0$, the extra contribution to the integral in (C.2) is easily determined. Further writing $J_{3/2}(ik)$ and $H_{3/2}^{(1)}(ik)$ in terms of modified Bessel functions, we obtain

$$\int_0^{\infty} \frac{dx}{x} \frac{J_{3/2}^2(x)}{(x^2+k^2)} = \frac{1}{3k^2}[1 - I_{3/2}(k) K_{3/2}(k)]. \tag{C.7}$$

However, $I_{3/2}(k) K_{3/2}(k) = (1+k)(k \cosh k - \sinh k)/k^3 \exp k$, (C.8)
from which the result for $S(\omega)$ quoted in (23) follows on simplification.

References

Balakrishnan V 1976 unpublished lecture notes
Buck O and Seeger A 1977 *Phys. Status Solidi* **A42** 285
Celasco M, Fiorillo F and Mazzetti P 1976 *Phys. Rev. Lett.* **36** 38 (referred to as CFM in the text)
Chadwick G A 1972 *Metallography of phase transformations* (London: Butterworths)
Dewel G, Walgraef D and Borckmann P 1977 *Z. Phys.* **B28** 235
Gardiner C W, McNeil K J, Walls D F and Matheson I S 1976 *J. Stat. Phys.* **14** 309
Gardiner C W 1976 *J. Stat. Phys.* **15** 451
Gittus J 1975 *Creep, viscoelasticity and creep fracture in solids* (London: Applied Science)
Grossmann S 1976 *J. Chem. Phys.* **65** 2007
Haken H 1977 *Synergetics* (New York: Springer-Verlag)
Janssen HK 1976 *Z. Phys.* **B23** 245
Kubo R 1966 *Rep. Prog. Phys.* **29** 255
Mazzetti P 1964 *Nuovo Cimento* **31** 88
Oberhettinger F 1972 *Tables of Bessel transforms* (New York: Springer-Verlag)
Prigogine I and Nicolis G 1977 *Self-organisation in non-equilibrium systems* (New York: Wiley-Interscience)
Rama Rao P 1978 private communication
Schilling W 1975 in Proceedings of the international conference on fundamental aspects of radiation damage in metals,, Gatlinburg, eds M T Robinson and F W Young (Springfield: U.S. Department of Commerce)
Schilling W 1977 in Proceedings of the Indo-German Seminar on Radiation Damage (Reactor Research Centre, Kalpakkam, Department of Atomic Energy)
Seeger A and Mehrer H 1970 in *Vacancies and interstitials in metals*, eds A Seeger, D Schumacher, W Schilling and J Diehl (Amsterdam: North-Holland)
Seeger A 1973 *Cryst. Lattice Defects* **4** 221
Seeger A 1975 in Proceedings of the Gatlinburg Conference, cited above
Van der Ziel A 1953 *Physica* **19** 742
Van Kampen N G 1977 in Topics in *Statistical mechanics and biophysics* ed R A Piccirelli (New York: American Institute of Physics)
Venkataraman G 1975, 1978 private communication
Venkataraman G and Balakrishnan V 1978 *Bull. Mater. Sci.* **1** 59
Watson G N 1928 *A treatise on the theory of Bessel functions* (Cambridge: University Press)
Wichert Th, Deicher M, Echt O and Recknagel E 1978 *Phys. Rev. Lett.* **41** 1659